Order and localization in randomly cross-linked polymer networks

Sandra J. Barsky and Michael Plischke
Physics Department, Simon Fraser University, Burnaby, British Columbia, Canada V5A 1S6
(Received 1 June 1995)

We study, by molecular dynamics, the onset of order and localization in randomly cross-linked polymer networks as the number n of cross links is increased. We find a well-defined critical number of cross links n_c above which the order parameter $q = 1/N \sum_i \langle |\exp i\mathbf{k} \cdot \mathbf{r}_i| \rangle^2$ increases as $q \sim (n - n_c)^\beta$, with $\beta \approx 0.5$ for $|\mathbf{k}| = 2\pi/L$, where L is the length of the computational cell. At the same critical number of cross links, particles in the network become localized around their mean positions. We find that the distribution of localization lengths $P(\xi)$ is a universal function when plotted in terms of a suitable scaled variable.

PACS number(s): 82.70.Gg, 78.30.Ly, 64.60.Ak

I. INTRODUCTION

In the process of vulcanization [1] a polymer melt is converted from a fluid to an amorphous solid with nonzero shear modulus. While the theory of the vulcanization transition has a long history [2], it is only in recent years that techniques developed in the context of spin-glass theory have been brought to bear on the problem of randomly cross-linked macromolecules, which, because of the presence of quenched random variables — the location of the cross links — shares some features with the spin-glass problem [3–5]. These new approaches make a number of specific predictions [5,6] for the properties of cross-linked macromolecules in the vicinity of the critical point and it is therefore of interest to study this transition both by experiment and by simulation of idealized models. While there is an extensive literature on computer simulations of both dense polymer melts and networks [7], relatively little is concerned with the properties of networks near the transition between the liquid and amorphous states.

In this paper, we report the results of molecular dynamics (MD) simulations of several systems consisting of relatively short polymer chains of mass $M = 10$ or $M = 20$. These chains were first equilibrated as a dense melt and then randomly cross linked with a fixed number n of bonds. The resulting network was again equilibrated and its properties determined in subsequent molecular dynamics runs. Because both macroscopic and microscopic properties are sensitive to the details of the connections, especially near the transition, all properties were averaged over 10 – 25 of different realizations of the cross linking. Because both long MD runs for each cross linking and many different cross linkings are required, we report here the results for rather small systems consisting of 250, 600, and 1000 monomers. Calculations on substantially larger systems are in progress and will be reported elsewhere.

In our calculations, we have attempted to determine the order parameter $q(n)$, the fraction of localized particles $Q(n)$, and the distribution of localization lengths $P(\xi, n)$ as a function of the number of cross links, n. The order parameter q is defined [4] in the following way:

$$q(n) = \frac{1}{N} \sum_i \left| \langle e^{i\mathbf{k}\cdot\mathbf{r}_i} \rangle \right|^2 , \tag{1.1}$$

where the angular brackets indicate averaging over a molecular dynamics run and the sum is over the N monomers comprising the system. This function clearly distinguishes between the liquid and amorphous states. If we take $\mathbf{k} = \frac{2\pi}{L} l(n_x, n_y, n_z)$, where the numbers n_α are integers and L is the length of the cubic computational box, then q is clearly zero in the liquid state in which each particle samples the entire volume, provided we avoid the trivial $\mathbf{k} = \mathbf{0}$ point. On the other hand, in the amorphous phase at least some of the particles are confined to a fraction of the computational box surrounding a mean position. Each of these particles contributes a nonzero value to the sum in (1.1), making this expression positive. Clearly, q is a function of $\mathbf{k}$ as well as of n. In our calculations, we have primarily used the three smallest symmetry-equivalent wave vectors of the form $\mathbf{k} = \frac{2\pi}{L}(1, 0, 0)$.

In order to obtain the distribution of localization lengths, we have in fact calculated the order parameter q_i for each of the particles in the system. We assume, and have verified for a number of samples, that in the rigid state the distribution in space of individual particles is described by a Gaussian probability density

$$\tilde{P}(\mathbf{r}_i) = \frac{1}{\pi^{3/2}\xi^{3/2}} \exp\left\{ -\frac{|\mathbf{r}_i - \bar{\mathbf{r}}_i|^2}{\xi_i^2} \right\} , \tag{1.2}$$

where $\bar{\mathbf{r}}_i$ is the mean position of this particle. The width of this distribution, ξ_i, is the localization length. The "order parameter" q_i is related to ξ_i by $q_i(\mathbf{k}) = \exp(-k^2\xi_i^2/2)$ and from this equation we may obtain the localization length ξ_i and a histogram of the function $P(\xi)$.

The fraction of localized particles is to some extent ambiguous in a calculation of finite length — not all delocalized particles will uniformly sample the entire computational box even in a very long MD run. Therefore,

we have arbitrarily defined Q in terms of the localization length. We calculate the fraction of particles with $\xi_i \leq L/4$ and take this fraction to be Q. The qualitative dependence of Q on the number of crosslinks is unaffected by the choice of $L/4$ as the cutoff.

In Sec. II we describe our model and computational techniques in more detail. Section III contains the results of these calculations and we conclude in IV with a discussion and outlook for future work.

II. THE MODEL

Our model of polymers is identical to one used in an extensive set of calculations by Kremer and Grest and collaborators [8]. All particles in the system interact through a truncated, purely repulsive Lennard-Jones potential

$$U_{\mathrm{LJ}}(r_{ij}) = \begin{cases} 4\epsilon\left[\left(\frac{\sigma}{r_{ij}}\right)^{12} - \left(\frac{\sigma}{r_{ij}}\right)^{6} + \frac{1}{4}\right], & r_{ij} < 2^{1/6}\sigma \\ 0, & r_{ij} \geq 2^{1/6}\sigma\,. \end{cases} \tag{2.1}$$

On a given chain consisting of M particles, neighboring particles are tethered to each other by means of the following potential [9]

$$U_{nn}(r_{ij}) = \begin{cases} -\frac{1}{2}kR_0^2 \ln\left[1 - \left(\frac{r_{ij}}{R_0}\right)^2\right], & r_{ij} < R_0 \\ \infty, & r_{ij} \geq R_0, \end{cases} \tag{2.2}$$

where $R_0 = 1.5\sigma$ and $k = 30\epsilon/\sigma^2$. The combination of these two potentials prevents polymers from passing through each other.

Our simulations consist of constant-energy molecular dynamics calculations. The equations were integrated with a standard velocity Verlet algorithm [10] with a time step adjusted to conserve energy to 1 part in 10^4 over the length of a run. All systems were first equilibrated as melts at a density of $\rho\sigma^3 = 0.85$ and an average temperature $k_BT = \epsilon$. For these parameters, there is a wealth of data available [8,11] with which we were able to compare the properties of our dense melts. In all cases, quantities like the end-to-end distance, radius of gyration, and eigenvalues of the moment of inertia tensor were consistent with values reported in the literature.

Once an equilibrated melt had been obtained, the chains were cross linked in the following way. A particle was selected at random and a neighborhood of radius 1.25σ was searched for other particles. Nearest-neighbor particles on the same chain were excluded and one of the remaining particles in the neighborhood was selected at random. The cross linking was then achieved by imposing the tethering potential (2.2) between these two particles. If no eligible particle was found in the neighborhood, a new central particle was chosen. The entire process was repeated until the desired number of cross links had been generated. We did not find it necessary to restrict the number of cross links per particle — even at the highest density of cross links it was rare that a given particle was linked to more than two others not on the same chain. Once the cross linking was complete, the average temperature was increased from ϵ/k_B to between $4\epsilon/k_B$ and $6\epsilon/k_B$ in order to speed up the sampling of configuration space. Although this requires the use of a smaller time step in the integration routine in order to guarantee energy conservation, it does save computer time.

The calculation of the order parameter (1.1) deserves some comment. Instead of using formula (1.1), one could calculate q from the expression

$$q = \frac{1}{N}\sum_i \left|\left\langle e^{i\mathbf{k}\cdot(\mathbf{r}_i - \bar{\mathbf{r}}_i)}\right\rangle\right|^2 ,$$

where $\bar{\mathbf{r}}_i$ is the mean position of particle i, which would have to be determined either in a separate MD run, or as part of the production run at the price of enormous cost in data storage. The disadvantage to (1.1) in the context of an MD calculation is that $q(t=0) = 1$ and its running average decreases as function of the integration time t. Since one is interested in the infinite-time limit of this and other quantities, it is necessary to extrapolate the results. We have found empirically that $q(t) \approx q(\infty) + a/\sqrt{t}$, at least initially for heavily cross-linked systems, and for very long times for systems close to the critical number of cross links. This is shown in Fig. 1 for a few samples, one quite close to the critical number of cross links. For heavily cross-linked systems we have run the MD calculations until the order parameter reached its equilibrium value; in other cases, we have extrapolated to $t = \infty$, recognizing that this extrapolation may result in a slight underestimate of $q(\infty)$. Clearly, the other quantities such as the average localization length and the fraction of localized particles can be extrapolated to $t = \infty$ in the same way. The determination of the probability distribution $P(\xi)$, on the other hand, must be done using the values of $q_i(t_f)$ at the end, t_f, of the production run. We have found that when plotted as a function of the

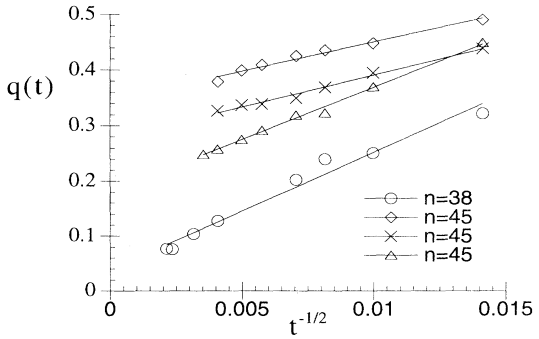

FIG. 1. Plot of the order parameter q as function of integration time for 25 polymers each of size $M = 10$. The critical number of cross links is between 37 and 38. The plot illustrates that $q(t) \approx q(\infty) + a/t^{0.5}$ and that $q(\infty)$ varies significantly between different realizations of the same number of cross links, even for $n = 45$, which is substantially larger than n_c.

scaled variable $\xi/\bar{\xi}(t_f)$ the distribution is insensitive to the value of t_f at least for the length of MD runs that we have used to generate our data.

III. RESULTS

In Figs. 2 and 3 we display the order parameter for 25 chains of length $M = 10$ and 30 chains of length $M = 20$. Also shown are fits to a power law of the form $q(n) = a(n - n_c)^{\beta_q}$ and $Q(n) = b(n - n_c)^{\beta_Q}$, where the parameter n_c was forced to be the same in both fits. In both cases, the exponents were found to be $\beta_q \approx 0.5$ and $\beta_Q \approx 0.4$, although we do not attach too much significance to these numbers since (i) the systems are rather small and (ii) there is at this point insufficient data in the critical region. We note that Castillo, Goldbart, and Zippelius [6] predict $Q \sim (n - n_c)$, i.e., $\beta_Q = 1$, consistent with the mean-field theory of percolation. As argued by de Gennes [12] and verified by Grest and Kremer [13], mean-field critical exponents provide an excellent description of the percolation transition of cross-linked polymers in the long-chain ($M \to \infty$) limit. Although our data are best fit with a considerably smaller exponent, the fit is dominated by points far from n_c and we cannot rule out a larger values of the exponents β_Q and β_q. We have also determined q and Q for the larger system of 100 polymers of length $M = 10$. The results are consistent with those shown in Figs. 2 and 3. In this case, the critical number of cross links is $n_c \approx 117$, suggesting that as the number of polymers is increased at fixed M, the critical number of cross links per polymer becomes smaller and closer to the value at which percolation occurs [13].

As mentioned above, we have also determined the distribution of localization lengths for all three of our systems. Castillo, Goldbart, and Zippelius [6] have predicted that the $P(\xi)$ is a universal function of the scaled localization length $\xi/\bar{\xi}$, where, in their theory, $\bar{\xi} \sim (n - n_c)^{-0.5}$ in the vicinity of the transition. In Fig. 4 we show this distribution for several values of n in the regime where most of the particles are localized plotted as function of the scaled variable $\xi/\bar{\xi}(n)$ and it is clear that the data indeed collapse to a single universal function for these parameters. An equally excellent collapse is shown in Fig. 5 for the smaller system of 250 particles. On this graph we have also plotted the universal function derived by Castillo, Goldbart, and Zippelius [6] with the location of the peak adjusted to correspond to that of our data. Clearly, the simulation data are not well described by this function for large ξ where $P(\xi)$ decays much more slowly than the theoretical curve.

Very close to the transition, the function $P(\xi)$ changes character, developing a secondary peak in the tail of the distribution. This is illustrated in Fig. 6 for two values of n close to n_c. It is noteworthy that the data again collapse to a single curve, indicating that for all cross linkings there is only one significant length, $\bar{\xi}$, in the system. The distribution is also remarkably insensitive to changes in N and the length of polymer. In Fig. 7 we plot one such curve for each of the three different systems that we have simulated. In each case $P(\xi)$ is taken from

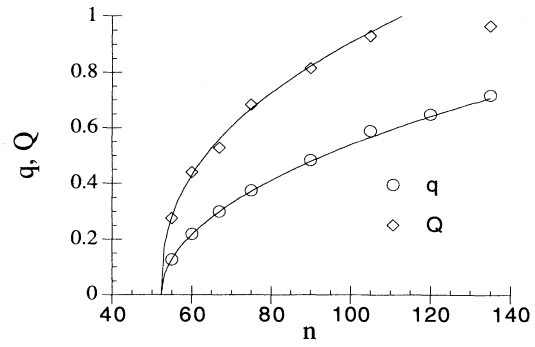

FIG. 3. Same as Fig. 2 for $M = 20$ and $N = 600$. The exponents are again given by $\beta_q = 0.5$ and $\beta_Q = 0.4$. The critical number of cross links $n_c \approx 52.3$.

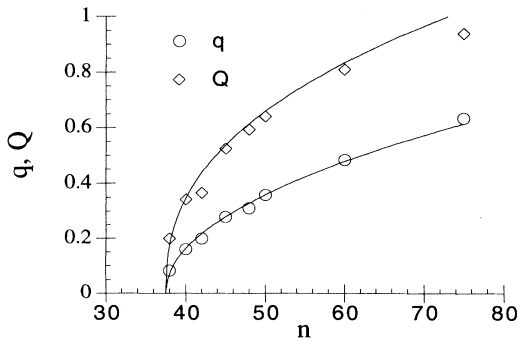

FIG. 2. The order parameter q and fraction of localized particles Q plotted against n for $M = 10$ and $N = 250$. The critical number of cross links n_c is estimated to be $n_c \approx 37.5$ and the curves are power-law fits with exponents $\beta_q = 0.5$ and $\beta_Q = 0.4$.

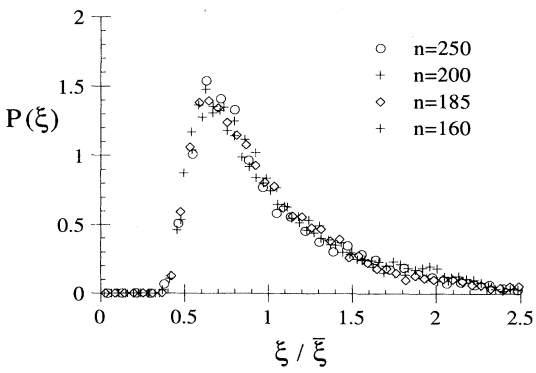

FIG. 4. Plot of the normalized distribution of localization lengths $P(\xi)$ as a function of the scaled variable $\xi/\bar{\xi}$ for 100 polymers of length $M = 10$ in the strongly cross-linked regime.

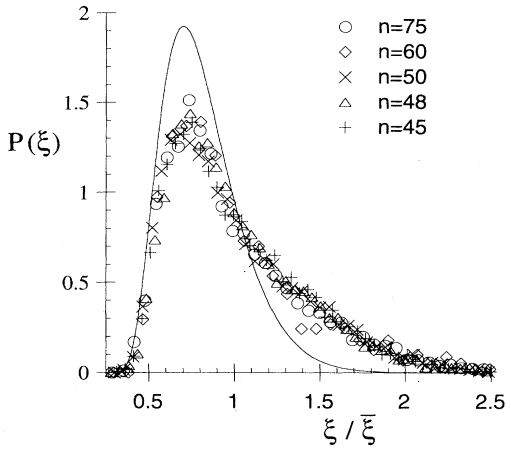

FIG. 5. Same as Fig. 4 for 25 polymers of length 10. Also shown is the universal probability density derived in [6].

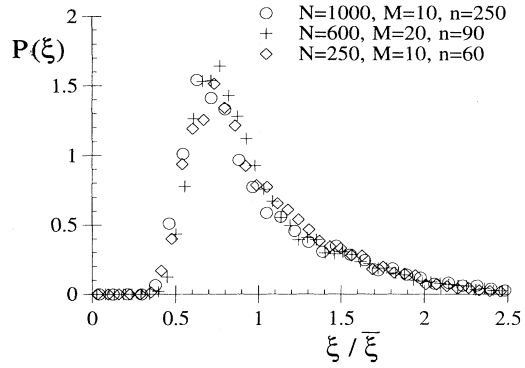

FIG. 7. Plot of $P(\xi)$ for $N = 250$, 600, and 1000 for $n \gg n_c$. The good agreement between the three sets of data is evidence that finite-size effects are minimal.

the regime in which most of the particles are localized. This collapse is less compelling in the critical region — the secondary peak at large ξ shifts to larger values of $\xi/\bar{\xi}$ as the number of polymers is increased.

We note that our calculation of the function $P(\xi)$ is different from that envisaged by Castillo, Goldbart, and Zippelius. In their formalism, only the fraction Q of localized particles is described by this distribution — there would be a second peak of weight $1 - Q$ at $\xi = \infty$ if the entire system were described in this way. We are unable to sharply distinguish between localized and free particles since $\sigma \leq \xi < L$, where L is the size of the computational box. Therefore, it is not surprising that our $P(\xi)$ is quite different from that of [6] in the critical region since our delocalized particles appear in the tail of $P(\xi)$ as well as in the secondary peak mentioned above. However, for the parameters used in Figs. 4 and 5 almost all particles are localized and we believe that the difference between the two functions cannot be accounted for by these considerations.

Finally, we show in Fig. 8 the average localization length as function of the number of cross links. All three systems display the same general behavior with $\bar{\xi}$ attaining a limiting value of roughly $0.35L$ at the critical point. For these systems this corresponds to $\bar{\xi}(n_c) \leq 1.75R_g$ where R_g is the average radius of gyration of the polymer in the melt. The theory of [6] is expected to be valid when $\bar{\xi} \gg R_g$ and our polymers are therefore not long enough to provide a test of this theory in its primary region of applicability. For large n it is possible to fit the data to a power law of the form $\bar{\xi}/L \sim (n - n_c)^{-\nu}$ but the value of ν is quite imprecise, ranging from 0.2 to 0.4, depending on what part of the data set is used.

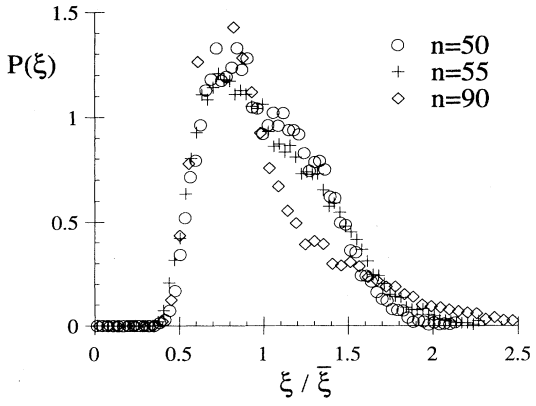

FIG. 6. The distribution of localization lengths for $n \approx n_c$ for 30 polymers of length $M = 20$. In this regime $P(\xi)$ develops a secondary peak at large ξ presumably due to the presence of a significant number of free particles. This peak shifts to larger values of ξ as N is increased.

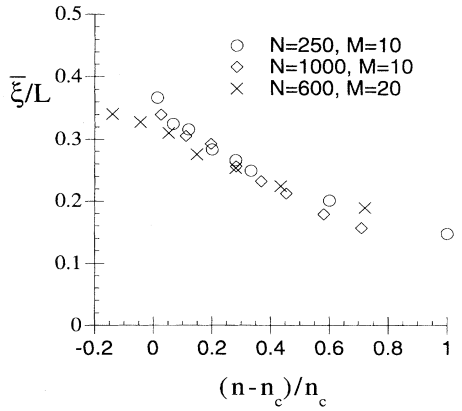

FIG. 8. The average localization length $\bar{\xi}$ plotted as a function of number of cross links for $N = 250$, 600, and 1000.

IV. DISCUSSION

In this first set of simulations, we have shown that the amorphous state of a randomly cross-linked polymer network with conserved topology is characterized by a universal distribution of localization lengths. This distribution seems to be largely insensitive to both the chain length and the system size, at least away from the critical region. This result is consistent with recent theoretical predictions although the shape of the universal function is substantially different from the predicted one [6]. We have also measured the order parameter and fraction of localized particles as function of number of cross links and found that both increase as q, $Q \sim (n - n_c)^\beta$, where β lies in the range $0.4 \leq \beta \leq 0.6$ for both quantities. This value of the exponent β is closer to the critical exponent for the gel fraction in three-dimensional percolation than it is to that predicted by mean-field theory or the tree approximation [12]. It remains to be determined whether or not this result will survive when more data in the critical region and results for larger values of N and M become available.

To better understand the vulcanization transition, many calculations remain to be carried out. Firstly, we are in the process of calculating the shear modulus for these systems. This is done by applying a simple shear and calculating the stress tensor as a function of the distortion [14]. The effects of conserved topology on the order parameter and the distribution of localization lengths can be investigated. We are exploring this by reducing the parameter σ in the repulsive Lennard-Jones potential close to zero, thus allowing the chains to cut through each other.

Finally, as mentioned in the Introduction, the cross links are quenched random variables similar to fixed random exchange interactions in spin glasses. One of the more intriguing aspects of spin glasses is the potential for replica-symmetry breaking [15] or ergodicity breaking. We have investigated the question of broken ergodicity for our systems using the method of Thirumalai, Mountain, and Kirkpatrick [16]. These authors showed that the time dependence of the so-called energy metric

$$d(t) = \frac{1}{N} \sum_{j=1}^{N} \left[\epsilon_{\alpha,j}(t) - \epsilon_{\beta,j}\right]^2 , \qquad (4.1)$$

where

$$\epsilon_{\alpha,j}(t) = \frac{1}{t} \int_0^t dt' E_{\alpha,j}(t')$$

is strikingly different in liquid and amorphous phases. Here the subscripts α, β refer, in their case, to different initial states of a mixture of two species of particles and $E_{\alpha,j}(t')$ is the energy of particle j in an N-particle system. They found that in the liquid state the function $d(t)$ decays to zero very rapidly whereas in a glassy state it reaches a plateau that decreases slowly on a much longer time scale, indicating the presence of energy barriers large enough to prevent the two systems from sampling the same region of phase space. The mixtures of Thirumalai, Mountain, and Kirkpatrick are different from our system in that there are no quenched random variables, analogous to our fixed cross links, in that case. We have calculated $d(t)$ for a number of different cross linkings both close to the transition and deep in the solid phase. In our calculations, the states α and β differed from each other by the assignment of initial velocities (same average energy). In all cases, the function $d(t)$ decays to zero within several hundred time steps, suggesting that phase space, for a given choice of cross linkings, is not sectioned. This may again be due to the fact that the chains are short — the amount of volume available to particles between two cross links is certainly not very large for chains of length 10 or 20 and one would expect any energy barriers to be small. Nevertheless, the issue of replica symmetry breaking or broken ergodicity is an important one and it will be interesting to investigate this for longer chains and by other methods such as the calculation of the overlap distribution $P(q_{\alpha\beta})$ of the order parameter [15].

ACKNOWLEDGEMENTS

We thank David Boal, Paul Goldbart, Gary Grest, and Bela Joos for helpful conversations and Paul Goldbart for comments on an earlier version of this manuscript. This research was supported by the NSERC of Canada.

[1] L.R.G. Treloar, *The Physics of Rubber Elasticity* (Clarendon, Oxford, 1975).
[2] P.J. Flory, *Principles of Polymer Chemistry* (Cornell University Press, Ithaca, 1953).
[3] R.T. Deam and S.F. Edwards, Philos. Trans. R. Soc. London A **280**, 317 (1976).
[4] P.M. Goldbart and N.D. Goldenfeld, Phys. Rev. Lett. **58**, 2676 (1987); Phys. Rev. A **39**, 1402 (1989); **39**, 1412 (1989); N.D. Goldenfeld and P.M. Goldbart, *ibid.* **45**, RC5343 (1992).
[5] P.M. Goldbart and A. Zippelius, Phys. Rev. Lett. **71**, 2256 (1993).
[6] H.C. Castillo, P.M. Goldbart, and A. Zippelius, Europhys. Lett. **28**, 519 (1994).
[7] For a recent review of this literature, see K. Kremer and G.S. Grest, in *Monte Carlo and Molecular Dynamics Simulations in Polymer Science*, edited by K. Binder (Clarendon Press, Oxford, 1994).
[8] K. Kremer and G.S. Grest, J. Chem. Phys. **92**, 5057 (1990); **94**, 4103 (1991); J. Chem. Soc. Faraday Trans.

88, 1707 (1992); E.R. Duering, K. Kremer, and G.S. Grest, Macromolecules **26**, 3241 (1993).
[9] R.B. Bird, R.C. Armstrong, and O. Hassager, *Dynamics of Polymeric Liquids* (Wiley, New York, 1977), Vol. 1.
[10] M.P. Allen and D.J. Tildesley, *Computer Simulation of Liquids* (Oxford University Press, New York, 1987).
[11] K. Kremer, G.S. Grest, and I. Carmesin, Phys. Rev. Lett. **61**, 566 (1988).
[12] P. G. de Gennes, J. Phys. Lett. (Paris) **38**, L-1 (1976).
[13] G.S. Grest and K. Kremer, J. Phys. (Paris) **51**, 2829 (1990).
[14] R. Everaers, K. Kremer, and G.S. Grest (unpublished). We are indebted to G.S. Grest for bringing this method to our attention.
[15] See, for example, M. Mezard, G. Parisi, and M.A. Virasoro, *Spin Glass Theory and Beyond* (World Scientific, Singapore, 1987).
[16] D. Thirumalai, R.D. Mountain, and T.R. Kirkpatrick, Phys. Rev. A **39**, 3563 (1989).